

Thermal Flow Analysis in Natural Gas Tubings In Relation To Downhole Applications

K.H. Al-Muhammadi¹, B.S. Yilbas^{2,3,4}, S.Z. Shuja², A. Al-Sharafi^{2,4}

¹EXPEC Advanced Research Center, Saudi Aramco, Dhahran, 31311, Saudi Arabia

²Mechanical Engineering Department, King Fahd University of Petroleum and Minerals, Dhahran, 31261, Saudi Arabia

³Center of Research Excellence in Renewable Energy (CoRE-RE), KFUPM, Dhahran, 31261, Saudi Arabia

⁴Senior Researcher at K.A. CARE Energy Research & Innovation Center at Dhahran, Saudi Arabia

Abstract - Tubing materials remain critical for gas wells because of the harsh downhole environments. The flow system in the tubing for downhole applications becomes critical for sustainable operation of the gas piping system. In the present study, gas flow system in relation downhole pipe applications is considered and flow and temperature variations in the tubing are simulated incorporating the geothermal data and the downhole conditions. A computer code developed and the COMSOL multi-physics code are used in the flow and temperature simulations. The findings revealed that the pressure drop and temperature variation along the tubing are high, which is associated with the frictional losses and the conduction heat transfer through piping to the environmental soil. The water constitute remains in liquid phase in the downhole conditions because of excessively high pressure. In addition, the pressure drop is not sufficient to create vapor phase of water in the pipe exiting region.

Keywords: gas-piping, pressure drop, heat transfer, downhole applications

1. Introduction

In gas flow systems, thermoplastic pipes find wide applications because of their mechanical and chemical properties, such as low density, high flexibility under bending forces, and high corrosion resistance. Some of the applications of reinforced thermoplastic materials in petroleum industry can possibly include sucker rod guides, anti-extrusion devices, electrical connectors, and a variety of other lightly loaded structures [1]. On the other hand, polyphenylene sulfide (PPS) and polyetheretherketone (PEEK) remain the most promising polymeric resins for downhole applications in oil and gas industry. This is mainly because of the superior properties of the semi-crystalline resin used in the piping systems; hence, the resin material does not absorb/contain excessive water while demonstrating strong chemical resistance at high operating temperatures. The resin material also provides required toughness and abrasion resistance at high ambient temperatures and pressures. Because of the high cost of such resins, their applications are limited in oil and gas industry. On the other hand, thermal-flow analysis in the gas tubing systems remains critical for downhole applications. This is because of the harsh downhole conditions, which causes increased gas temperature and pressure in the downhole. This, in turn, limits the selection and use of thermal plastic piping materials for gas transport from downhole conditions. Consequently, assessment of temperature and pressure variation in the piping system becomes necessary for sustainable operations.

Several studies were carried out exploring the gas flow characteristics in piping system. Deng et al. [2] introduced a numerical investigation to observe the most affecting parameters on heat and mass transfer during wax deposition in piping system operation. In addition, they also introduced quantitative study analyzing the heat and mass transfer during the process. Their findings reveal that the increasing trend of wax deposition was observed with an increasing gas flow rates under the regime of oil-gas stratified pipe flow. Kesana et al. [3] reported new sets of data on streamwise droplet velocity profiles for low liquid loading pipe flows. In the analysis, instantaneous streamwise velocity data were obtained using the non-intrusive Laser Doppler Anemometry (LDA) technique. Later, the data were used to calculate mean and root-mean-squared (RMS) local velocities. They showed that irrespective of the conditions studied, the single-phase gas flow characteristics were preserved closer to the top pipe wall. The data from the LDA implied that the bottom pipe half region was highly influenced by the gas-liquid interfacial characteristics. This resulted in high streamwise turbulence intensity. Zang et al. [4] studied three-dimensional Eulerian model combined with the kinetic theory of granular flow (KTGF) to simulate the gas-liquid-solid flow with the presence of gas hydride dissociation. They indicated that the continuous production of gas bubbles by

gas hydrate (GH) dissociation lead to more violent fluctuations in the pressure gradient and a more marked elevation of the solid particles compared with the liquid–solid two-phase flow without GH dissociation. In addition, the effect of GH dissociation on the multiphase flow under different hydrate saturations was analyzed. Behbahani-Nejad et al. [5] introduced a new formulation for isothermal gas flow in a pipeline with gravity and friction source terms and solved by finite element methods using FEniCS open-source computing platform. The findings revealed that, even with large time-step and coarse mesh, the predictions were in good agreement with those obtained with a fine mesh. Zou et al. [6] interpreted slugging flow, which was the most common flow regime in a pipeline-riser system. In the context of non-uniformity, the findings differed from the approaches used to characterize slugging cycles in the early studies. Their findings might contribute to a better and more specific understanding of gas/liquid flow mechanisms in a pipeline-riser system. In addition, it could serve as means to evaluate the features of laboratory pipeline-riser systems. Vasques et al. [7] studied the interfacial wave structure of the liquid film in both upward and downward annular gas-liquid flows in an 11.7 mm size pipe. The investigations were conducted using the Brightness Based Laser Induced Fluorescence technique (BBLIF). It was shown that more liquid travels in the base film in upwards flow, which was consistent with the base film thickness measurements. The role of gravity was much more important on the base film than on disturbance waves. Omar et al. [8] attempted to assess the suitability of several correlations specifying to slug flow regime for a fluid pair that was different to air-water system. They demonstrated that the flow development beyond 45D (D being the tubing diameter) had minimal effect on the slug flow regime. The change in physical properties of the liquid phase was found to be responsible for the deviation associated with the existing slug flow models, particularly those developed to predict the gas holdup in liquid slugs. Birvalski et al. [9] conducted an experimental investigation for assessing the flow characteristics of stratified wavy flow of air and water through a horizontal pipe. They showed that the wave patterns were consisted of gravity and gravity-capillary waves, respectively, with substantial differences in the wave characteristics and liquid velocities. Contrary to this, the effect of the waves on the gas velocities was rather similar in both wave regimes while causing an increase in the velocity fluctuations close to the interface. Kadri et al. [10] investigated the effect of gas pulsation at the pipeline inlet on the length and frequency of long slugs for gas–liquid flow in horizontal pipelines. The results showed that a strong relation was present between the frequency of gas pulsation and the resulting slug flow. Particularly gas pulsation could decrease the size of the long liquid slugs significantly. Yu et al. [11] investigated the characteristics of gas–liquid annular and stratified flow through a horizontal pipe while using the two-phase hydrokinetics theory. Since the model study was less dependent on the specific empirical apparatus and data, it formed the foundation for further establishing a flow measurement model of wet gas which would produce fewer biases in the results when it was extrapolated. Hallanger et al. [12] introduced a computational fluid dynamics (CFD) analysis that was performed to understand the characteristics in a gas export metering station at an offshore installation on the Norwegian Continental Shelf. They demonstrated that both the pipe geometry upstream the inlet header and the geometry of the inlet header itself might affect the flow profile in the flow meters. El-Askary et al. [13] examined the effects of solid-particles on downward turbulent-air flow through a pipe with sudden expansion via introducing the Eulerian–Lagrangian approach. It was shown that the finest particles could improve the performance of the sudden expansion, while the size of separated bubbles increased. Zhu et al. [14] investigated numerically a three-dimensional drill pipe-casing annulus including drill pipe connector. Based on the analysis of calculated flow characteristics, a structure optimized scheme by reducing the slope of drill pipe connector was put forward to decrease the erosion rate and increased the life of drill pipe. Aliyu et al. [15] presented an experimental study on the flow behavior of gas and liquid in the upward section of a vertical pipe system with an internal diameter of 101.6 mm and a serpentine geometry. The qualitative and statistical analyses showed that the new correlation provided improved predictions for two-phase flow film thickness in large-diameter pipes. Andrianto et al. [16] examined the transient behavior of gas-liquid plug two-phase flow in a horizontal pipe. They conducted CFD simulations and experiments on the transient behavior of two-phase flow in the piping system. The results provided a quantitative agreement between calculations and experimental data for the elongated bubble length and the time variation of the liquid hold-up.

In general, most of the published works deal with multi-phase flow including liquid-gas or gas-particle flow [2 – 16]. Multi species of gas flow, such as mixture with different concentration of gases/liquids are not much visible in the open literature. On the other hand, because of high cost of thermoplastic materials, their applications become limited particularly in oil and gas industries. One of the alternative cost-effective materials for tubing is Polyvinylidene fluoride (PVDF). This

is because of PVDF material, which is one of the high molecular weight fluorocarbons having superior properties against abrasion and mechanical loads. Tubing material is expected to demonstrate high abrasion resistance, dielectric properties, and mechanical strength at large temperature ranges within -40°C to 121°C depending on the downhole applications. This in turn makes the thermal flow analysis in tubing being critical for natural gas flow in downhole applications. Hence, in the present study, thermal flow in tubing is simulated while mimicking the downhole gas reservoir conditions. Since the natural gas composes of various constitutes, in the analysis this issue is considered and typical gas composition is incorporated in the analysis. In addition, a typical volume flow rates for gas reservoir is used together with the tubing and downhole configurations including lining sizes, geothermal data, and down hole pressure and temperature. Since the tubing length exists over two kilometers, first, the resistance method is used to determine temperature variation along the tubing length via superimposing the solution obtained from each tube segments, and later pressure drop in the tube is evaluated from coupling of thermal filed in the energy equation. It is worth to mention that in the energy equation, gas hydrostatic effect and tubing frictional losses are also incorporated. The study is extended to include numerical simulation using the commercial code, COMSOL, for segmented tubes. In this case, the tubes are divided into several segments and the flow properties obtained from the simulation data are superimposed to the inlet boundary conditions of the next consecutive segment. Findings are compared with those obtain from the resistance method.

2. Analysis of Flow and Thermal System

Thermal flow analysis of the natural gas flow through the downhole tubing is carried out incorporating the mass, momentum and energy balance. Since the pipe length is extremely long (over 7000 feet), the numerical simulation using the commercial codes, such as COMSOL, becomes difficult because of the required grids size, which is estimated well excess of ten billion grids points. Consequently, a computer code is developed considering the flow and heat transfer analogy. In this case, the pipes are divided into segments and the flow properties obtained from the simulation data are superimposed to the inlet boundary conditions of the next consecutive segment.

The properties of natural gas compose of various constitutes are incorporated. In addition, the pipe and the lining sizes, geothermal data, and down hole pressure and temperature are included in the analysis. In the thermal analysis, two approaches are incorporated including the resistance method and COMSOL simulations. In the resistance method, temperature variation along the pipe length is formulated via superimposing the solution obtained from each tube segment. Later pressure drop in the tube is evaluated from coupling of thermal filed in the energy equation. In the energy equation, the gas hydrostatic effect and tubing frictional losses are incorporated. Fig. 1 depicts the schematic view of resistance system incorporated in the thermal analysis.

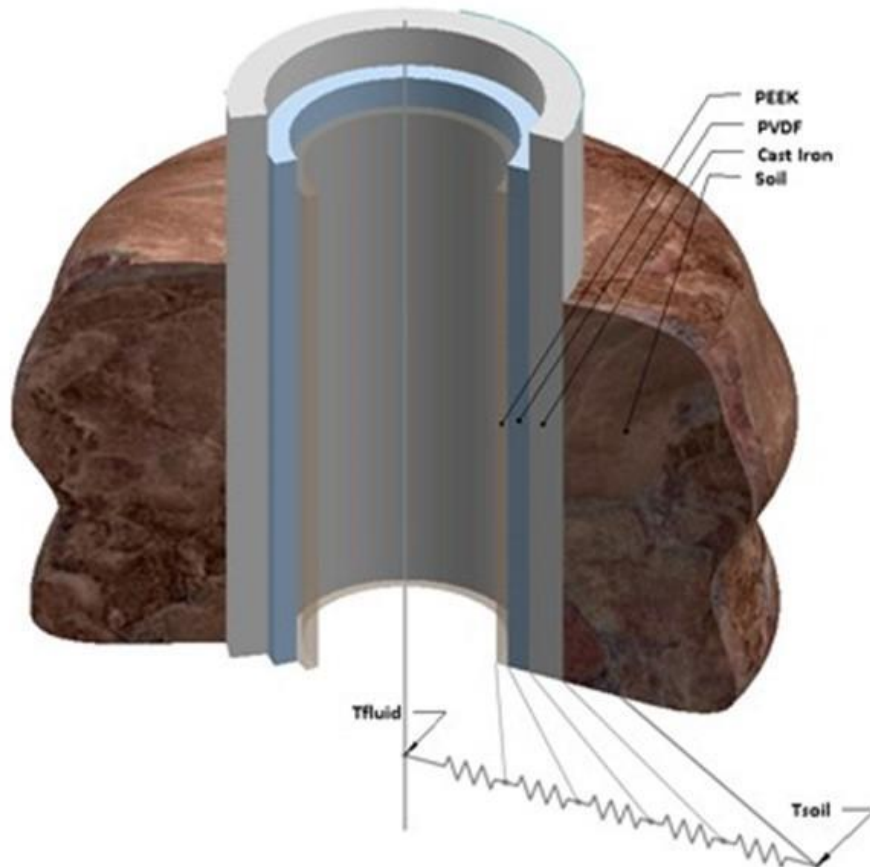


Fig. 1: A schematic view of tube cross-section with resistance system incorporated in the analysis.

The data for the tube cross-section (Fig. 1) is given in Table 1. The gas composition used in the analysis given in Table 2. Moreover, the gas mixture properties are assessed using the mixture equations.

Table 1. Gas composition in the downhole (% mass ratio).

	Mass fraction (m_f)
H ₂ S	0.06
CO ₂	0.05
H ₂ O	0.1
CH ₄	0.79

Table 2. Data related to the tube cross-section sizing.

Soil thickness	50 inch
Pipe outer Diameter	4.5 inch
Pipe thickness	0.6 inch
PVDF Layer thickness	0.5 inch
PEEK Layer thickness	0.0197 inch

The mixture properties of the gas at temperature T and pressure P can be written as:

$$\begin{aligned}
 N_i &= \frac{m_{fi}}{M_i} \\
 N_m(t) &= \sum_n N_i \\
 y_i &= \frac{N_i}{N_m}; \quad P_i = Py_i
 \end{aligned} \tag{1}$$

where i represents the species in the mixture and N corresponds to molar ratio of constituting gas specie. Temperature and pressure dependent properties can be obtained from EES program, i.e.: $C_{pi}(T), \rho_i(T, P_i), k_i(T), Pr_i(T), \mu_i(T)$. Therefore, the fluid properties yield:

$$C_{pm} = \sum_n m_{fi} C_{pi}; \quad \rho_m = \sum_n m_{fi} \rho_i; \quad k_m = \sum_n m_{fi} k_i; \quad Pr_m = \sum_n m_{fi} Pr_i; \quad \mu_m = \sum_n m_{fi} \mu_i \tag{2}$$

On the other hand, the equations governing the resistance method satisfying the energy, momentum, and mass balance are briskly described below. The total flow length of the tube L is divided into N segments from inlet to outlet and the length of each segment becomes: $\Delta L = L/N$. The fluid mixture properties at a local temperature T_{fluid} and local pressure can be determined from Eq. 2. This allows to determine the Reynolds number, since mass flow rate and cross-sectional area of tube

are known ($A_{flow} = \frac{\pi D_{inner}^2}{4}$, here Dinner is the inner diameter of the tune) i.e.

$$Re = \frac{\rho V D_4}{\mu} \tag{3}$$

The friction factor and the Nusselt number can be determined from the relation: $Nu = fn(Re, Pr) = \frac{h D_4}{k}$; $f = fn(Re, \Delta L / D_4, \varepsilon / D_4)$. Here D_i is the outer diameter of the tube casing (steel), and D_4 is the inner diameter of PEEK (Fig. 1).

The thermal resistance between the fluid and tube inner surface (Fig. (1)) can be written as:

$$R_4 = \frac{1}{h\pi D_4 \Delta L} \quad (4)$$

Here, h is the heat transfer coefficient, D_4 is the PEEK inner diameter (Fig. 1). The radial thermal resistance for diameters of liners inside the tube D_1 to D_3 (here D_3 is the PVDF inner diameter) is the along the element of length ΔL can be written as:

$$R_{i(0-3)} = \frac{\ln(D_i / D_{i+1})}{2\pi(\Delta L)k_i} \quad (5)$$

and the overall resistance is:

$$R_{tot} = \sum_{i=0-4} R_i \quad (6)$$

The heat loss from the segment is:

$$Q_{loss} = \frac{T_{fluid} - T_{soil}}{R_{tot}} \quad (7)$$

where T_{fluid} is fluid temperature at the segment inlet and T_{soil} is the temperature around the surrounding soil. However, heat loss associated with the fluid over ΔL segment length is:

$$Q_{loss} = \dot{m}C_p (T_{f,inlet} - T_{f,outlet}) \quad (8)$$

$T_{f,inlet}$ and $T_{f,outlet}$ are the fluid temperature at segment inlet and segment exit over the segment length ΔL .

The soil and thermal conductivity of tube and lining material can be obtained from EES data. Thermal conductivities of soil and steel casing of tubing are considered to be temperature dependent while thermal conductivity of lining materials considered to be constant.

The pressure loss along the segment length obeys the Darcy law; hence, the pressure loss along the segment length ΔL can be determined according to:

$$\Delta P_{loss} = f \frac{\Delta L}{D_4} \frac{\rho V^2}{2} + \rho g \Delta L \quad (9)$$

The following formulations are applicable for all segments considered (N) along the tube length (L).

The flow inside the tubing (Fig. 1) is also simulated using COMSOL Multiphysics code to assess temperature and pressure distribution inside the tubing. Since, the flow is turbulent inside the tubing, k- ω turbulence model is incorporated. The boundary conditions adopted in the resistance method are incorporated in the numerical simulations. At the inner surface of PEEK, which is between the flow and PEEK inner surface, no-slip and conjugate heating conditions (continuity of temperature and heat flux) are incorporated. In addition, at each interface of the tubing, continuity of temperature and heat flux are adopted. The solution domain of the tube segment is set to be same for that of considered in the resistance method.

The fine grids are located in the region close to PEEK inner wall, where the rate of fluid strain is large in the viscous sub-layer.

3. Results and Discussion

Flow and temperature analysis of the downhole tubing system is considered and simulation of flow system is realized incorporating the downhole conditions. In addition, the predictions of temperature and pressure data are extended using the Fanno and Rayleigh line approaches.

Table 3 gives temperature and pressure predicted from the resistance simulations. In addition, results obtained from Fanno and Rayleigh Line approaches are also provided in Table 3 for comparison. It is worth to mention that Fanno and Rayleigh line flows calculations, same heat transfer and tubing resistance data are used, which are used in the resistance analysis. The pressure prediction using the Darcy–Weisbach approach while adopting the heat transfer via resistance method remains slightly lower than that obtained from Fanno and Rayleigh line flows. This because of the fact that Fanno line flow omits the heat transfer and incorporates the fluid friction in the tubing while Rayleigh line flow only considered the heat transfer from the downhole gas to the surrounding soil environment and neglects the fluid friction. Hence, assumption of heat transfer or pipe friction only fails the correct predictions of the pressure drop. Moreover, temperature predicted, due to heat transfer along the 7000 ft pipe, is the lowest for Rayleigh line flow, and then follows the wire method and the Fanno line flow. It is worth to note that although the Rayleigh line flow considers the heat transfer unlike Fanno flow, the energy dissipation due to fluid friction is not accounted for. Hence, fluid friction contributes to the temperature rise in the flow system while enhancing the fluid temperature at the tubing exit. Consequently, fluid friction contributes to the temperature drop along the tubing.

Table 3 Temperature and pressure data predicted from resistance, Fanno and Rayleigh Line flow analyses. T_{exit} and P_{exit} represents the gas temperature and pressure at the tube exit.

	Using mixture	Using Methane	
	Resistance Method	Fanno Line	Rayleigh Line
P_{exit} (Pa)	2.99E+07	3.4380E+07	3.45E+07
T_{exit} (K)	351.4	393	342.6

In order to observe temperature distribution along the tube segment incorporated in the wire method, numerical simulations are also considered using COMSOL code. The flow properties are kept same as those used in the resistance method. The simulation data for temperature and velocity distributions are shown in Figs 2a and 2b. The frictional losses around the PEEK inner causes a shear layer in the wall vicinity. Since the gas flow system is considered, the low viscosity of the fluid gives rise to thin shear layer close to the PEEK inner surface. However, the shear layer thickens towards the outlet of the pipe segment (Fig. 2a). This, in turn, results in relatively larger viscous dissipation towards the segment exit. Since the flow is subsonic in the pipe, the heat transfer from gas to its surrounding through the tubing contributes to flow acceleration inside the tubing. In addition, friction within the pipe contributes to flow acceleration in the tubing because the subsonic nature of the flow. Hence, contribution of both fluid friction and heat transfer to the flow acceleration contributes to velocity increase in the gas and the pressure drop. In the case of temperature distribution inside the tubing segment (Fig. 2b), temperature reduces slightly close to the inner diameter of PEEK, which is because of low thermal conductivity of PEEK and PVDF used in the lining of the cast iron pipe. In addition, the friction layer generated in the close region of PEEK inner wall contributes to the fluid temperature in the gas. This contribution remains small as compared to convective heat loss from tubing to the surrounding soil. Hence, temperature variation in the gas across the tube segment becomes small. However, high temperature region does not extend excessive in the soil because the low thermal conductivity of the soil surrounding

of the tubing outer diameter (cast iron pipe outer diameter). Nevertheless, temperature predictions are in-agreement with that obtained from the resistance method. Although thermal flow analysis in the tubing for downhole applications is extensively carried out, improvement of PVDF material thermal properties, such as thermal conductivity remains important, which is left for the future study.

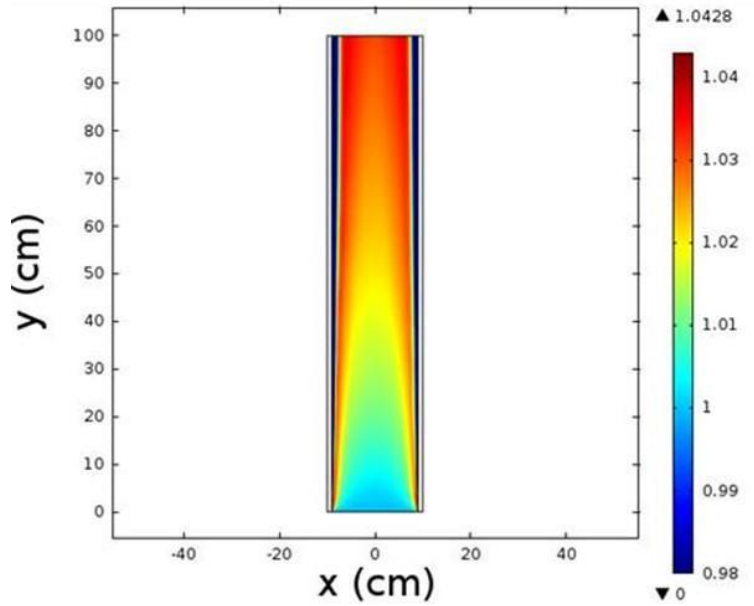


Fig. 2a: Velocity contours inside tube segment. Velocity is in m/s.

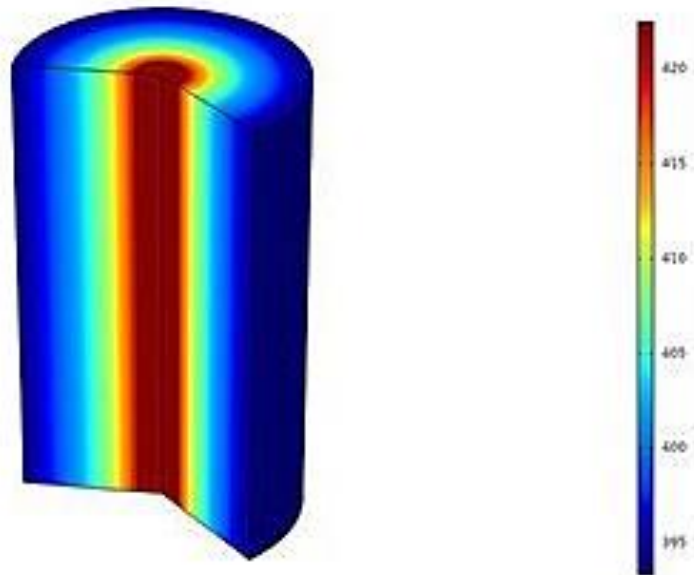


Fig. 2b: Temperature contours inside tube segment. Temperature is in K.

4. Conclusion

Thermal flow analysis pertinent to gas piping and the flow system for oil-gas downhole applications is presented. The tubing materials considered consist of cast iron pipe (outer tubing) PEEK and PVDF materials (lining inside cast iron pipe), which are found to be suitable for such applications. The thermal analysis incorporating the heat transfer and fluid flow is incorporated and the resistance method is used to simulate flow and thermal properties via segmenting the tube along the 7000 ft tubing. The tube segment is simulated to verify the resistance predictions using the COMSOL software. COMSOL predictions for temperature agree well with the data obtained from the resistance analogy. In addition, temperature predictions obtained from the resistance method are compared to those obtained from the classical approaches using the flow formulations basing on Fanno and Rayleigh lines. The findings reveal that Fanno and Rayleigh line predictions over estimate temperature and pressure of the gas at the tubing exit. This is because of the coupled heat transfer with the flow resistance along the tube, which are decoupled in Fanno and Rayleigh line flows. Heat convective and conduction transfer in the gas flow system give rise to temperature drop inside the tubing. However, due to the low thermal conductivity of PVDF and PEEK lowers the heat conduction from the gas towards the surrounding soil. The shear layer developed in the vicinity of PEEK inner wall causes pressure drop across the tubing. Since the gas flow is subsonic, heat transfer from gas to tubing surroundings soil as well as fluid friction in the tubing contributes to flow acceleration. This further lowers the pressure drop in the tubing; hence, the prediction of resistance method differs from the findings of Fanno and Rayleigh line flow. The present study explores the pressure and temperature drop in tubing system relevant to downhole gas-piping and provides useful information about the importance of tube lining.

References

- [1] K. Yu, E. V. Morozov, M. A. Ashraf, and K. Shankar, "A review of the design and analysis of reinforced thermoplastic pipes for offshore applications," *J. Reinf. Plast. Compos.*, vol. 36, no. 20, pp. 1514–1530, 2017.
- [2] J. Duan, S. Deng, S. Xu, H. Liu, M. Chen, and J. Gong, "The effect of gas flow rate on the wax deposition in oil-gas stratified pipe flow," *J. Pet. Sci. Eng.*, pp. 539–547, 2018.
- [3] N. R. Kesana, R. Ibarra, M. Langsholt, R. Skartlien, O. Skjæraasen, and M. Tutkun, "Measurements of local droplet velocities in horizontal gas-liquid pipe flow with low liquid loading," *J. Pet. Sci. Eng.*, vol. 170, pp. 184–196, 2018.
- [4] P. Li, X. Zhang, and X. Lu, "Three-dimensional Eulerian modeling of gas-liquid-solid flow with gas hydrate dissociation in a vertical pipe," *Chem. Eng. Sci.*, vol. 196, pp. 145–165, 2019.
- [5] M. Behbahani-Nejad, A. Bermúdez, and M. Shabani, "Finite element solution of a new formulation for gas flow in a pipe with source terms," *J. Nat. Gas Sci. Eng.*, vol. 61, no. November 2018, pp. 237–250, 2019.
- [6] S. Zou, T. Yao, L. Guo, W. Li, Q. Wu, H. Zhou, C. Xie, W. Liu, S. Kuang, "Non-uniformity of gas/liquid flow in a riser and impact of operation and pipe configuration on slugging characteristics," *Exp. Therm. Fluid Sci.*, vol. 96, pp. 329–346, 2018.
- [7] J. Vasques, A. Cherdantsev, M. Cherdantsev, S. Isaenkov, and D. Hann, "Comparison of disturbance wave parameters with flow orientation in vertical annular gas-liquid flows in a small pipe," *Exp. Therm. Fluid Sci.*, vol. 97, pp. 484–501, 2018.
- [8] R. Omar, B. Hewakandamby, A. Azzi, and B. Azzopardi, "Fluid structure behaviour in gas-oil two-phase flow in a moderately large diameter vertical pipe," *Chem. Eng. Sci.*, vol. 187, pp. 377–390, 2018.
- [9] M. Birvalski, M. J. Tummers, and R. A. W. M. Henkes, "Measurements of gravity and gravity-capillary waves in horizontal gas-liquid pipe flow using PIV in both phases," *Int. J. Multiph. Flow*, vol. 87, pp. 102–113, 2016.
- [10] U. Kadri, R. A. W. M. Henkes, R. F. Mudde, and R. V. A. Oliemans, "Effect of gas pulsation on long slugs in horizontal gas-liquid pipe flow," *Int. J. Multiph. Flow*, vol. 37, no. 9, pp. 1120–1128, 2011.
- [11] P. Yu, Y. Li, J. Wei, Y. Xu, and T. Zhang, "Modeling the pressure drop of wet gas in horizontal pipe," *Chinese J. Chem. Eng.*, vol. 25, no. 7, pp. 829–837, 2017.
- [12] A. Hallanger, C. Saetre, and K. E. Frøysa, "Flow profile effects due to pipe geometry in an export gas metering station – Analysis by CFD simulations," *Flow Meas. Instrum.*, vol. 61, pp. 56–65, 2018.
- [13] W. A. El-Askary, I. M. Eldesoky, O. Saleh, S. M. El-Behery, and A. S. Dawood, "Behavior of downward turbulent gas-solid flow through sudden expansion pipe," *Powder Technol.*, vol. 291, pp. 351–365, 2016.

- [14] H. Zhu, Y. Lin, D. Zeng, Y. Zhou, J. Xie, and Y. Wu, "Numerical analysis of flow erosion on drill pipe in gas drilling," *Eng. Fail. Anal.*, vol. 22, pp. 83–91, 2012.
- [15] A. M. Aliyu, A. A. Almbrok, Y. D. Baba, L. Lao, H. Yeung, and K. C. Kim, "Upward gas–liquid two-phase flow after a U-bend in a large-diameter serpentine pipe," *Int. J. Heat Mass Transf.*, vol. 108, pp. 784–800, 2017.
- [16] Deendarlianto, M. Andrianto, A. Widyaparaga, O. Dinaryanto, Khasani, and Indarto, "CFD Studies on the gas-liquid plug two-phase flow in a horizontal pipe," *J. Pet. Sci. Eng.*, vol. 147, pp. 779–787, 2016.